INTERNATIONAL ATOMIC ENERGY AGENCY
UNITED NATIONS EDUCATIONAL, SCIENTIFIC AND CULTURAL ORGANIZATION
INTERNATIONAL CENTRE FOR THEORETICAL PHYSICS
I.C.T.P., P.O. BOX 586, 34100 TRIESTE, ITALY. CABLE CENTRATOM TRIESTE

UNITED NATIONS INDUSTRIAL DEVELOPMENT ORGANIZATION

INTERNATIONAL CENTRE FOR SCIENCE AND HIGH TECHNOLOGY

SMR.550 - 10

SPRING COLLEGE IN MATERIALS SCIENCE ON

"NUCLEATION, GROWTH AND SEGREGATION IN MATERIALS

SCIENCE AND ENGINEERING"

(6 May - 7 June 1991)

STABILITY OF MICROSCOPIC CLUSTERS

(PART I)

J.A. ALONSO
Departamento de Fisica Teorica y Fisica Atomica y Nuclear
Facultad de Ciencias
Universidad de Valladolid
Valladolid
Spain

STABILITY OF MICROSCOPIC CLUSTERS

1st. Lecture: Introduction to clusters

J.A. ALONSO

Lectures to be delivered at:
Spring College in Materials Science on
"Nucleation, growth and segregation in Materials Science and Engineering"
(International Centre for Theoretical Physics, Triestre, May-June 1991)

1. INTRODUCTION

The names cluster or small particle are used for an aggregate containing from a few atoms up to a few thousand atoms. Due to their small size the properties of the clusters are often different from those of the corresponding bulk material. Studying the behavior of clusters one expects to obtain information on the early stages of the growth of matter. Typical questions which arise are: How many atoms a cluster of a metallic element must contain for developing metallic properties?, or, how properties like the geometric structure and melting temperature change with cluster size? (see Fig. 1). These and other similar questions have motivated the development of experimental techniques for producing small clusters as well as a series of experimental and theoretical studies of their properties. The key to explain many properties of clusters is the large surface to volume ratio. The existence of especially stable clusters is often advocated to construct models of amorphous systems. Going back to Figure 1, the growth process of clusters centres on two key questions:

a) How far does one have to follow the growth spiral before it becomes trivial to do so?

b) Before becoming trivial, what properties and laws does one encounter along the spiral? (By definition, they will be different from those known from macroscopic samples or from gases).

2. EXPERIMENTAL PRODUCTION

2.1 Clusters in matrices

Chemical reaction in a liquid medium[1]

Until now several procedures have been used for obtaining small particles through chemical reaction. In Table 1 we show some of them.

These procedures vary from simple precipitations to chemical reductions, including hydrolysis processes, thermal decompositions, etc. For example, the procedure for obtaining FeB magnetic particles consists in the reduction of Fe^{2+} salts using borohydride ions in aqueous solution. The simplified outline of the procedure followed is shown in Fig. 2. Parameters which affect the final characteristics of the particles are: 1) Speed of addition of reactives; 2) Atmosphere under which the reaction is carried out; 3) concentration of reactives, pH and temperature at which the reaction is carried out.

In order to control the growth of the particles and fix their final size so that one can obtain ultrafine quasi-monodisperse particles, several procedures have been developed. All of these are based on carrying out the chemical reaction in a microstructured medium. Among the different procedures we must highlight the one based on microemulsions. The size of the droplets in the microemulsion can be easily controlled. In this way, quasi-monodispersec particles can be obtained (with diameters in the nm scale; 1nm = 10^{-9}m).

Irradiation

Irradiation of a LiF crystal with neutrons produces different types of defects in the crystal, for instance interstitial Li atoms. When the irradiation dose is large enough (> 3 x 10^{21} neutrons/m^2) the Li atoms tend to form clusters.

Immersion of a porous glass into a liquid metal

Some inorganic glasses based on SiO_2 contain cavities with a diameter of up to 30 nm. When the porous glass is immersed in a molten metal and pressure is applied (7000 Torr), then metal droplets

enter the small pores.

The minerals known as Zeolites contain natural microscopic cavities which can easily accomodate metallic clusters. Fe aggregates trapped into the pores of silica minerals and zeolites form the basis of some commercial catalysts (for the production of hydrocabons starting from CO and H_2). Other aggregates in zeolites catalyze the polymerization of ethylene to give polyethylene.

Condensation on a substrate

A metallic vapor produced in an oven is condensed on a substrate (NaCl, or a metallic oxide). In this way, thin films formed by clusters can be obtained. The clusters are stabilized by maintaining the substrate cold. The production of thin films of aggregates with the right electronic properties would be of great interest for the microelectronics industry. The field is still in its infancy but one can anticipate applications in optical memories, image processing and superconductivity. The possibility to build parts of circuits with small aggregates would allow the fabrication of electronic devices at a molecular scale.

With the technique called Molecular Beam Epitaxy it is today possible to produce crystalline semiconductor superlattices of great precision. Use of clusters, instead of atoms, would allow the production of much more complex superstructures. A great effort is being dedicated to deposit clusters to produce superconductiong thin films (for instance Cu, Y and Ba oxides).

2.2 Clusters in gas phase

Liquid Metal Ion Source (LMIS)

The schematic of the experimental apparatus[2] used to produce Rb_N^+ clusters is shown in Fig. 3. This is a capillary-type LMIS. The metal is placed in the oven. By differential heating, Rb is distilled into the tungsten capillary needle which is itself heated to keep Rb in the liquid state. A high electric field is stablished between the tip of the capillary needle and a stainless-steel extraction electrode (E). Copious field emission of ions results when the potential difference between the tungsten needle and the extractor exceeds 2KV. The electrostatic lens assembly collimates the ion beam. Multiply charged clusters have also been obtained by this technique.

Ion Bombardment[3]

A primary beam, formed by noble gas ions (for instance Xenon ions of 10 KeV energy) hits the sample sheet (spot size 1mm in diameter) removing cluster ions. In this way, Katakuse and coworkers have obtained cluster ions (posivite and negative) of the noble metal group and Zn group[4]. Sputtering by ion beam bombardment of solid surfaces is a relatively cheap and simple means for the production of neutral, positively and negatively charged clusters even from materials with high melting temperature.

Ion-induced erosion is now explained by collission cascades originating from the impacts of single primary ions. All authors agree that a cluster stems from atoms of a collision cascade excited by a single projectile. Disagreement exists, however, whether entire clusters leave the surface with the atoms originating from neighboring lattice sites or wheather cluster formation is a

statistical recombination process of independently sputtered atoms from one collision cascade. Table 2 gives the sputtering yield Y (average number of emitted particles per projectile atom) and the maximum number of atoms, N_{max}, in sputtered positively charged cluster ions for several elements.

A typical sputtering apparatus is shown in Fig. 4. The part on the right side contains the primary ion source and the target device including acceleration and focussing optics. The sputtered ions are used to perform experiments on the left part of the Figure.

Supersonic nozzle sources[5]

Fig. 5 shows the main chamber of the supersonic nozzle source used in obtaining alkali clusters. The nozzle is a 0.0076 cm diameter hole with a 0.015 cm long channel. the nozzle is mounted at the end of a nozzle tube, the other end of which is connected to the reservoir. High purity metal is melted and introduced into the reservoir through a heated inlet pipe. The source and nozzle are further heated so that the desired metal vapor pressure (50-300 Torr) is obtained. The nozzle is kept about 100 K hotter than the reservoir to prevent plugging. The vapor then freely expands into the vacuum. The density and temperature of the jet decrease rapidly. Clusters form both in the nozzle channel and in the region justs outside. The product P_oD is a controlling parameter. P_o is the metal vapor pressure and D is the nozzle diameter. For small values of P_oD (larger, however, than a threshold value) most aggregates are produced in the throat. For larger values of P_oD, progressively more clusters are produced outside the nozzle.

The pure vapor sources produce some medium sized clusters but with very low abundances. This source is not ideally suited for the formation of large clusters because the vapor must act also as a heat bath to cool the clusters. Notice that the process of atom aggregation leaves the cluster in an excited state.

Seeded nozzle sources[5]

In a seeded jet source, an inert gas is mixed with a low concentration of a seed (e.g. alkali metal vapor), and the mixture is ejected. If the seed can condense, clusters will be formed in the expansion. This situation differs from the pure vapor expansion in that the carrier gas can serve as a heat bath for the seed. The fact that the carrier is an inert gas guarantees that it does not react with the seed. When the vapor pressure is high enough, collisions between seed and seed facilitates the equilibrium among the cluster species in the nozzle channel. The carrier gas mediates the equilibration and absorbs most of the heat of formation, which is converted into translational energy of the beam. Although the seeded-cluster source is a simple and reliable method of producing small and medium-size clusters, its operation requires rather high vapor pressure, and hence it is unsuitable for high-boiling-point metals.

Gas aggregation sources[5]

In the nozzle, the metal vapor exists in the supersaturated state for a relatively short time, and large clusters are not formed abundantly. The corresponding times in gas aggregation sources are longer, and large clusters are easily formed. One type of gas aggregation source is constructed as in Fig. 6. The metal vapor from

the oven enters the cool condensation chamber, where it mixes with a stream of inert gas at pressure of ≈ 1 Torr and temperatures of ≈ 77K. Cluster formation continues until the gas-cluster mixture is discharged through an orifice into a surrounding vacuum chamber. The size distribution is controlled by the temperatures of oven and condensation chamber and by the gas flow rate. This technique may be adjusted to produce clusters up to sizes containing 10^5 atoms.

Laser vaporization

This method was developed in 1981 by R.E. Smalley (Rice University) and V.E. Bondybey (ATT Laboratories). The technique can produce aggregates of up to 100 or more atoms of any substance which exists in the solid state (even the most refractory metals).

A pulsed laser baeam, carefully collimated, hits a metallic rod or disk (see Fig. 7) placed in a tube. The laser pulse evaporates atoms, producing an extremely hot plasma. This vapor is cooled by a stream of He gas flowing through that tube. This leads to condensation of the vapor and produces clusters of different sizes. The flowing current brings the clusters to a vacuum chamber where the pressure difference induces a supersonic expansion of the cluster beam. Collisions ocurring during this expansion cool the aggregates down to a low temperature. Both neutral and ionized clusters are obtained.

3. TYPES OF CLUSTERS

One can classify clusters according to the type of chemical bonding between the atoms forming the cluster (see Table 3, taken from ref. 6).

Van der Waals clusters

Interatomic interactions between inert gas atoms involve a central pair force which is extremely well known and so these clusters are popular with theorists. The low melting and boiling points of inert gases (derived from their weak interatomic binding) makes them equally attractive to experimentalists. The simple central forces imply that the most stable clusters will be the ones with high density, that is, with close-packing of atoms. Apart from the academic interest in inert gas clusters, these can form inside cavities in metals during ion beam mixing experiments[7]. In these experiments inert gas ions with a high kinetic energy are used to induce mixing of metallic multilayers to obtain amorphous alloys.

Metallic clusters

In Metals the interatomic forces are not simple. Many elemental metals are not close-packed, since the interatomic forces are partially directional. Both at the cluster level and at the macroscopic (bulk) level one can distinguish between simple metallic elements (Na, Al, etc) and transition metals (Fe, Co, etc), with some polyvalent non transition metals, like Pb forming a group in between. A lot of progress, both from the theoretical and experimental sides, has been achieved during the last years for simple metal clusters.

Network clusters

Covalent bonding is the dominating factor leading to network formation in clusters of some materials like Si, Ge and C. This also occurs in the corresponding crystals as well as in the amorphous forms of these elements. Most of the atoms in microclusters are at surface sites and have dangling bonds. These bonds may reform or

reconstruct, as is known to be the case for the surfaces of crystalline diamond, Si or Ge. How important can we expect this reconstruction to be in clusters?

Ionic clusters

Take NaCl, or CuBr as examples. These clusters are composed of spherical closed-shell ions (for instance Na^+ and Cl^-). The cohesion is due to monopole coulomb forces. The growth spiral of figure 1 shows in detail the picture one has for the first thirteen steps in the development of clusters of NaCl, or more correctly $Na^+(NaCl)_N$ with one excess sodium atom. One sees that the embryonic growth, which comes from a theoretical calculation[8], appears to terminate with the thirteenth cluster, which essentially is identical with the unit cell of the macroscopic crystal. In general, however, the development of bulk structure is not so simple.

Molecular clusters

These are typical of organic molecules and some closed-shell molecules like I_2.

Hydrogen-bonded clusters

These are formed by closed-shell molecules containing H and electronegative elements.

4. MASS ANALYSIS

When clusters have been produced by any of the methods presented in section 2, a distribution of sizes is obtained, that is, clusters with different number of atoms are generated in the same

experiment. The first task of the experimentalist is then to analyze the size distribution. This is achieved with a mass spectrometer. Before entering the mass spectrometer the clusters of the beam must be ionized. For this one can use laser ionization or electron beam ionization. Notice also that some of the experimental techniques of Section 2 already produce ionized clusters.

In the Time of Flight spectrometer a voltage pulse V accelerates all singly charged ions (q=1) into the same kinetic energy $qV = 1/2\ mv^2$. The mass-dependent velocity $v = (2q\ V/m)^{1/2}$ results in distinguishable flight times t for the different clusters, to reach a distance L where the detector is placed

$$t = \frac{L}{v} = L\left(\frac{m}{2\ qV}\right)^{1/2} \qquad (1)$$

5. VAN DER WAALS CLUSTERS

Cluster distributions obtained by Echt, Sattler and Recknagel[9] in Konstanz are given in figure 8 for the case of Xe. It is immediately apparent that the abundances vary in rather peculiar ways - the same each time the experiment is repeated. The abundance is not at all a monotonic function of size. Certain sizes are formed with high abundance, with the following few being especially rare. The breaks at size 13, 55 and 147 are particularly interesting. These numbers are elements of a series

$$N = 1 + \sum_{p=1}^{n} \left\{ 10\ p^2 + 2 \right\} \qquad (2)$$

with n = 1, 2 and 3 respectively. This series describes the packing of spheres in a family of closed icosahedral arrangements, named after Mackay[10]. Figure 9 gives the first five icosahedra Notice the pentagonal symmetry characteristic of an icosahedron. The interior atoms of the icosahedra are 12 fold coordinated, just as in a close-packed lattice. In subsequent experiments[11] the Konstanz group was able to show that breaks also occurred at the three following magic numbers 309, 561 and 923, corresponding to n = 4, 5 and 6 in eq. (2). And this is not all! Additional experiments for other Van der Waals clusters (Ar, Kr, CO, CH_4) show the same set of magic numbers, as the data included in Table 4 indicates (see also fig. 10 where we show the mass spectrum of large Ar clusters). CO and CH_4 are molecules for which a structure similar to that of rare gas clusters is most likely, because of the low anisotropy of their intermolecular interaction potentials. Whith reference to Table 4 notice that the study of CO and NH_4 clusters was restricted to sizes N<400.

This could hardly be accidental. Indeed diffraction experiments show that the diffraction pattern from clusters coming from a nozzle agreed with icosahedral packing, for a broad size range[12].

Once this becomes clear, it is possible to understand the remaining breaks in the spectra of figure 8, as steps towards the completion of a full shell. For example, the break at size 19 results from adding an extra pentagonal pyramid, with six atoms, onto the N = 13 cluster (figure 11).

The special stability of closed-shell icosahedral clusters is substantiated by theoretical calculations[13]. Fig. 12 gives the energy (per atom) of icosahedral clusters calculated by the Mie potential. The icosahedra with filled shells are characterized by relative energy

minima. A similar conclusion is reached from the calculated sublimation energies (figure 13). The difference in the sublimation energies of N =13 and N = 14 indicates that evaporative cooling of hot clustes will enhance the population of magic clusters.

Cluster growth occurs in phases in terms of packing of spheres adjacent to each other. Each phase terminates with the completion of a Mackay icosahedron. There are also subdivisions to each phase. A detailed analysis of these subdivisions is provided in the paper by Phillips[14]. The five-fold symmetric icosahedra, with shells arranged like shells in an onion around a central atom, are foreing to the crystallographer. Regular macroscopic crystals do not have shell structure. They do not possess a central atom. Quite the contrary, they are built from unit cells arranged like bricks in a three-dimensional linear lattice. The embryonic growth of rare gas clusters continues beyond one thousand atoms with no sign of a metamorphosis to a regular, translation invariant, macroscopic crystal structure.

There are speculations that a transition to the usual crystal structure occurs at a cluster size below 10.000. This occurs because hard spheres can not really be packed into the icosahedral structure such that adjacent spheres are touching each other. The spheres have to be soft. Then it is possible, but the inner spheres will be closer to each other than the spheres in the outer layers. As a result strain builds up in the cluster and at some stage it becomes favourable to release the strain through rearrangement of the atoms leading to the familiar structure of the macroscopic crystal[15]. Figure 14 shows how this is possible through a small displacement of the atoms. Electron diffraction patterns of free, neutral clusters feature extra lines which are incompatible with icosahedral structure for n >750 (ref.12).

Boyer and Broughton[15] have recently performed molecular dynamics simulations for clusters of up to N ≈ 5000 atoms interacting via Lennard-Jones potentials, which represent well the interaction between rare gases. Static energies for single-crystal fcc clusters, with varying surface structures, were computed and compared with those of icosahedral structures. The icosahedral form was found to have the lowest static energy for clusters of a few thousand atoms of fewer. The critical cluster size where the zero temperature free energy of the fcc structure becomes lower than that of the icosahedral structure is not easily determined, the main reason being that the energy of fcc clusters is sensitive to the surface structure and this one is difficult to determine for such large clusters.

As pointed out above the observed magic numbers are interpreted in terms of an enhanced thermodynamic stability of particularly compact structures. An interesting point about the mass spectra of figures 8 and 10 is that these correspond to ionized clusters. Ionization of small Van der Waals clusters by electron impact is accompanied by strong fragmentation and evaporative cooling. Consequently, the magic numbers observed reflect the intrinsic stability of charged clusters. This fact can explain some small anomalies in Table 4. Ionization of the cluster results in the formation of a dimer ion (e.g. Ar_2^+). Failure to observe pronounced features at N = 13 and 55 for Kr or CH_4 is most likely related to loss of stability by the distortion induced by the contraction of the interatomic separation in the molecular ion. In larger clusters, however, the (charged) defect is less likely to break the global structure, i.e. the geometrical arrangement of the atoms (or molecules) in the outer coordination shells. The magic numbers might, however, be shifted by one unit if the molecular ion is strongly contracted.

REFERENCES

1. M.A. Lopez-Quintela and J. Rivas, in "Structure, dynamics and equilibrium properties of colloidal systems", Ed, E. Wyn-Jones, Kluwer, Dordrecht (to be published)
2. N.D. Bhaskar, R.P. Frueholz, C.M. Klimcak and R.A. Cook, Phys Rev. B36, 4418 (1987)
3. K. Meiwes-Broer, in "Advances in metal and semicondutor clusters", Vol 1. Ed. M. Duncan, J.A.I. Press Inc, (1991); To be published
4. I. Katakuse , T. Ichihara, Y. Fujita, T. Matsuo, T. Sakurai and H. Matsuda, Int. J. Mass Spectrom. Ion Proc. 74, 33 (1986)
5. W.A. de Heer, W.D. Knight, M.Y. Chou and M.L. Cohen, Solid State Phys. 40, 93 (1987)
6. J. Jortner, D. Scharf and U. Landman, in "Elemental and Molecular Clusters". Ed. G. Benedek, T.P. Martin and G. Pacchioni, Springer Series in Materials Science, Vol 6 (1988), p. 148
7. D.R.G. Mitchell, S.E. Donnelly and J.H. Evans, Philos. Mag. A61, 53 (1990)
8. T. P. Martin, Angew. Chem. Int. Ed. Engl. 25, 197 (1986)
9. O. Echt, K. Sattler and E. Recknagel, Phys. Rev. Lett 47, 1121 (1981)
10. A. L. Mackay, Acta Crystall. 15, 916 (1962)
11. O. Echt, O. Kandler, T. Leisner, W. Miehle and E. Recknagel, J. Chem. Soc. Faraday Transact. 86, 2411 (1990)
12. J. Farges, M.F. de Feraudy, B. Raoult and G. Torchet, J. Chem. Phys. 84, 3491 (1986)
13. J.G. Allpress and J. Sanders, Aust. J. Phys. 23, 23 (1970)
14. J.C. Phillips. Chem. Rev. 86, 619 (1986)
15. L.L. Boyer and J.Q. Broughton, Phys. Rev. B42, 11461 (1990)

CAPTIONS OF FIGURES

Figure1. When a solid material is divided in small pieces and these in smaller pieces, etc., a point is reached when the aggregate only contains a few atoms. The properties of the cluster then differ considerably from those of the macroscopic solid. In particular the geometric structure can differ from that of a piece of the solid with the same number of atoms.

Figure 2. Flow diagram showing the production of fine Fe-B particles by chemical reduction.

Figure 3. Schematic of the experimental apparatus to obtain Rb_N^+ clusters by the Liquid Metal Ion Source technique.

Figure 4. Setup of the experiment on sputtered cluster ions. Charged clusters emerging grom the solid target (right side) are shaped into an ion beam, mass selected and subject to experimental investigations (left side).

Figure 5. Supersonic nozzle source chamber

Figure 6. Gas aggregation source.

Figure 7. Principle of the Laser Vaporization source. A pulsed high-energy laser light produces a plasma which is entrained in a pulsed He beam.

Figure 8. Mass spectrum of Xenon clusters obtained in a supersonic expansion of Xenon gas through a fine nozzle into vacuum.

Figura 9. Mackay icosahedra. The number of spheres in each cluster is (for increasing size) : 13, 55, 147, 309 and 561.

Figure 10. Mass spectrum of large Ar clusters, indicating icosahedral shell structure at N = 561 and 923.

Figure 11. This is the structure of the icosahedron. A stable cluster with N = 19 is obtained by adding and extra pentagonal pyramid, with six atoms, to this cluster.

Figure 12. Calculated cohesive energy of icosahedral clusters.

Figure 13. Calculated sublimation energy for Ar clusters

Figure 14. Transition from icosahedron (a) to cuboctahedron (b). By pulling the corners as indicated by the arrows it is possible to shift the icosahedral structure into a cuboctahedron.

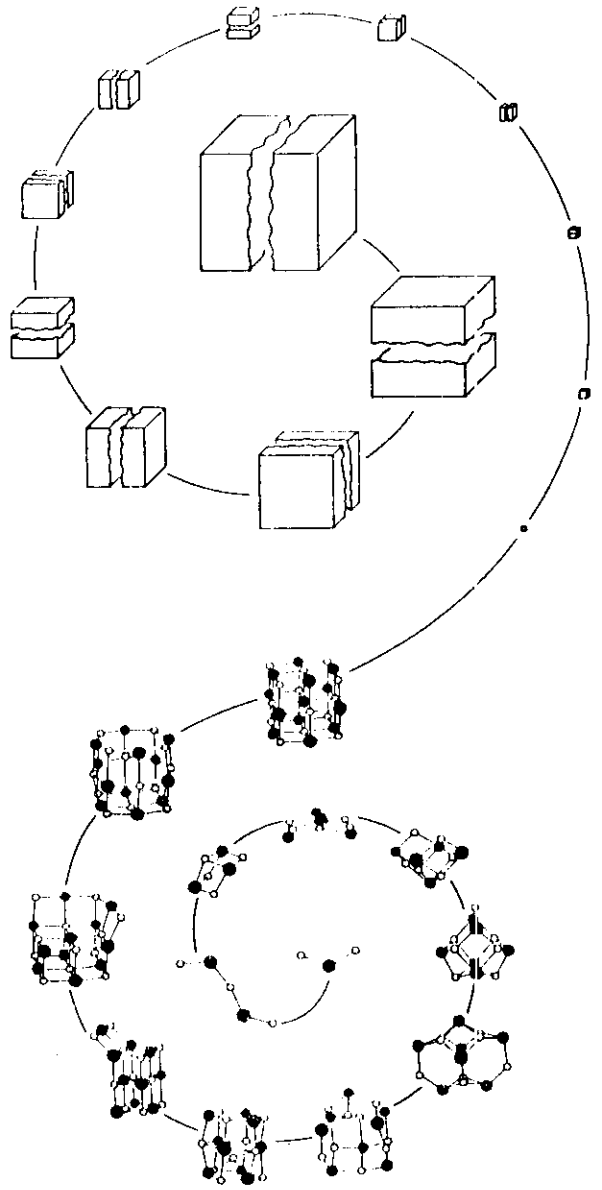

Fig. 1

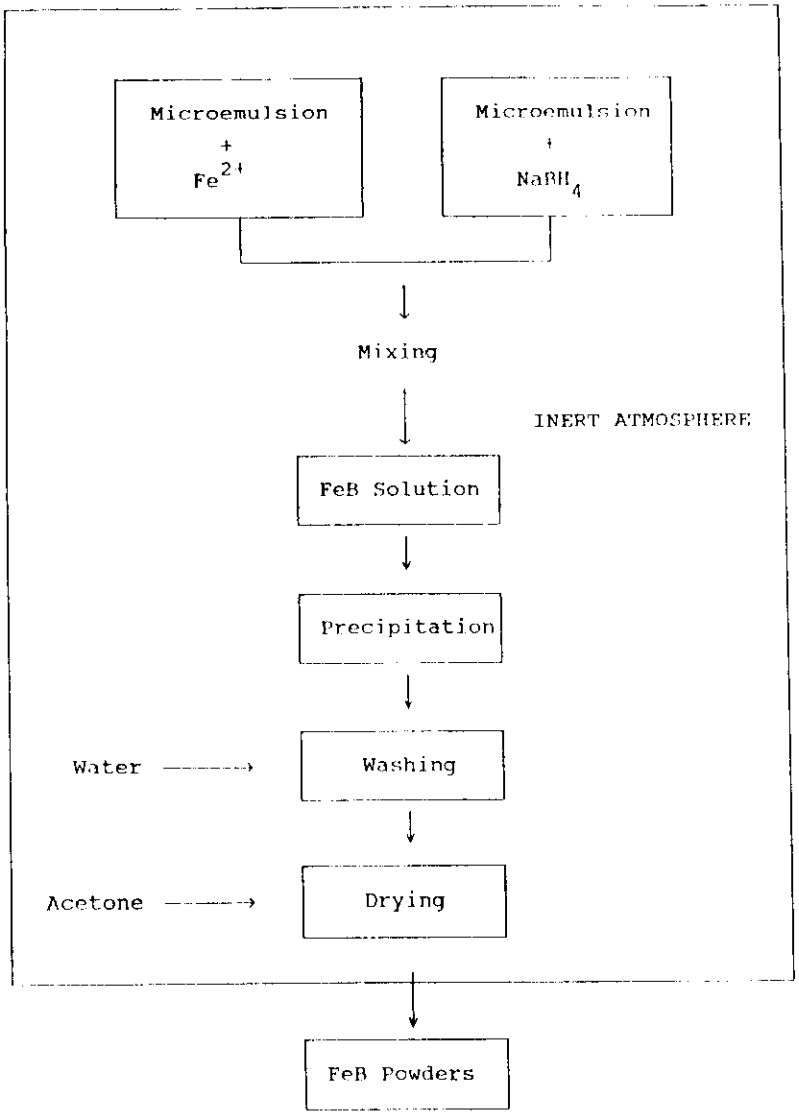

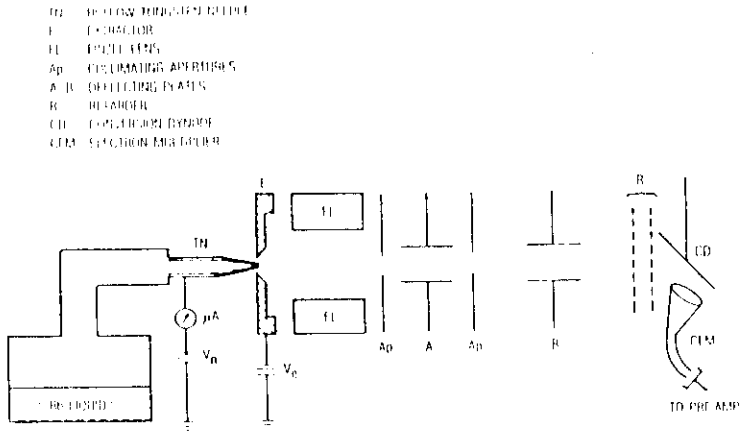

FIGURE 2 . Flow diagram showing the production of fine Fe-B particles by chemical reduction.

Fig 3

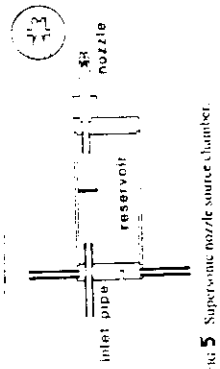

Fig. 5 Supersonic nozzle source chamber.

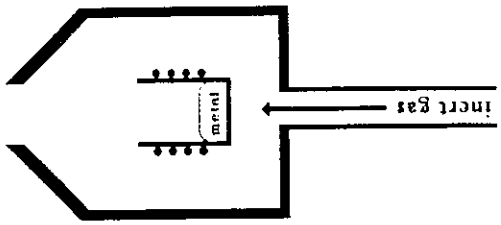

Fig. 6 Gas sputtering source

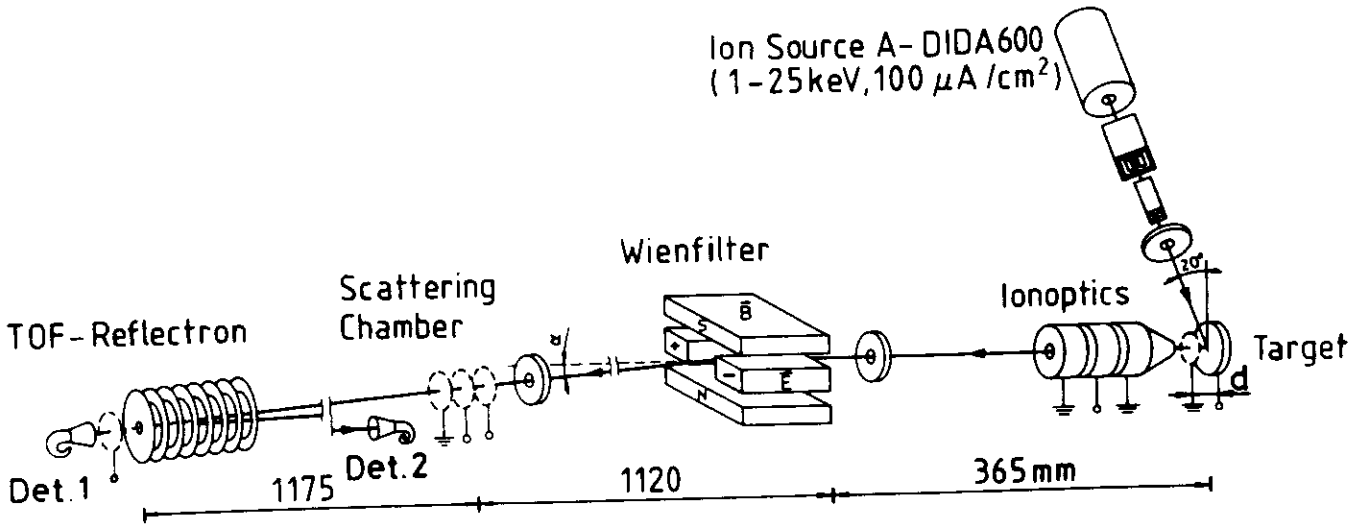

Fig. 4

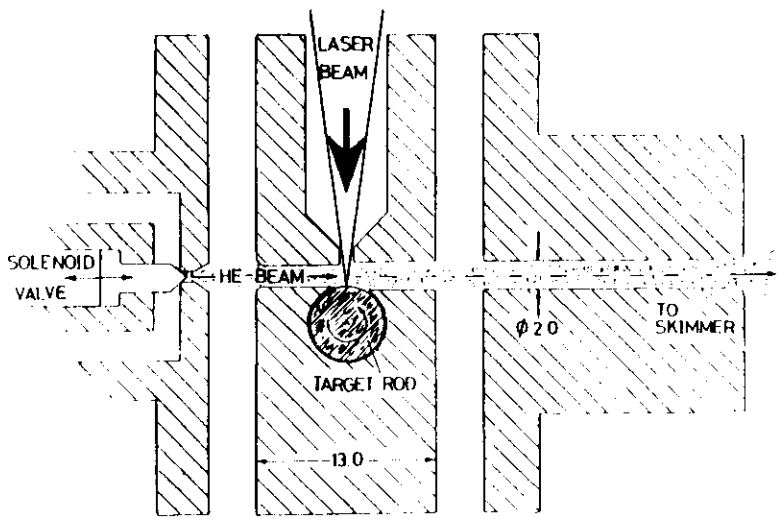

Fig. 7

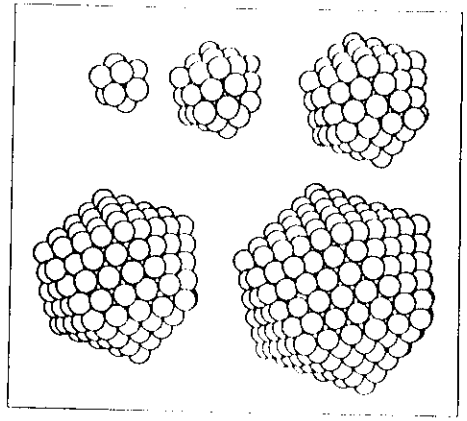

Figure 9 Mackay icosahedra. From top-left to bottom-right the number of spheres in each cluster are 13, 55, 147, 309 and 561, respectively.

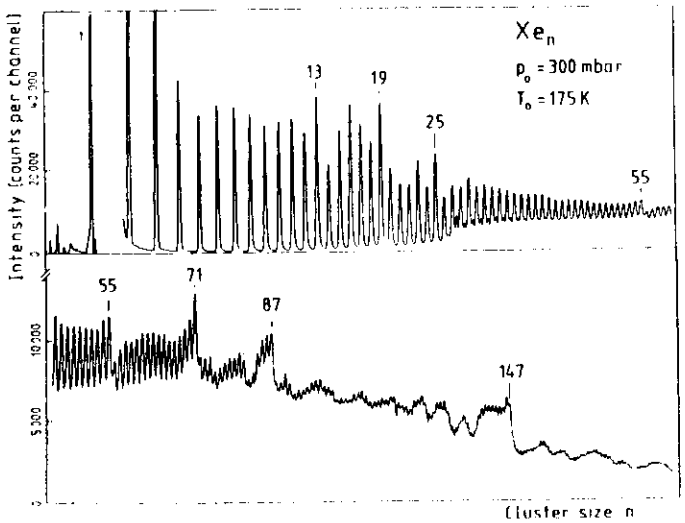

Figure 8. Concentration profile of Xe clusters produced by adiabatic expansion and ionized by an electron beam.

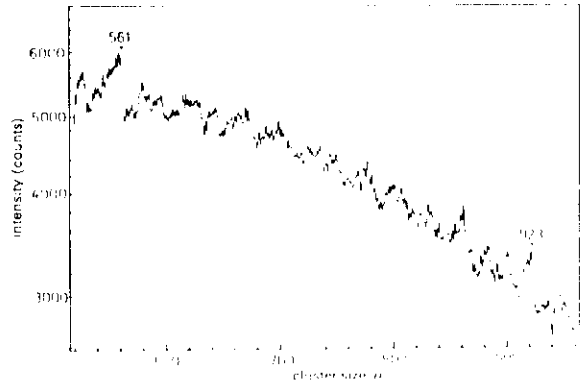

Fig. 10 Mass spectrum of large Ar clusters, indicating icosahedral shell closure at n = 561 and 923.

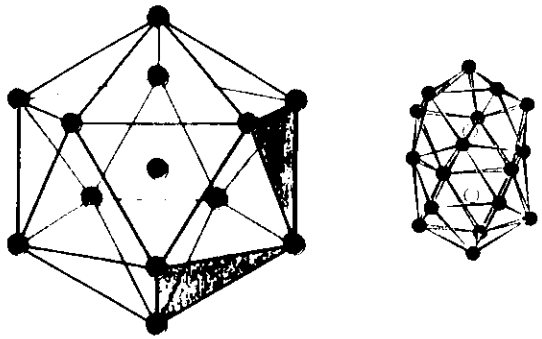

Fig. 11

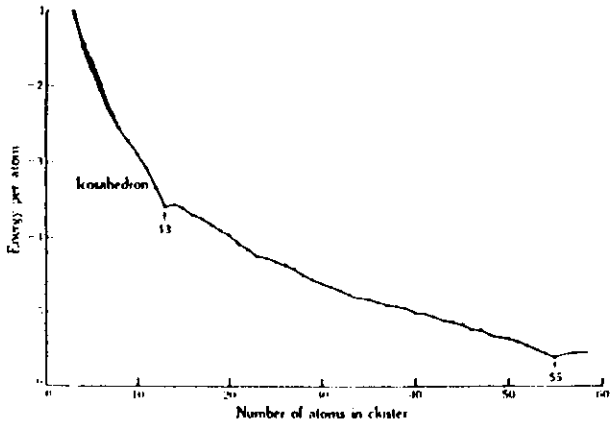

Fig. 12

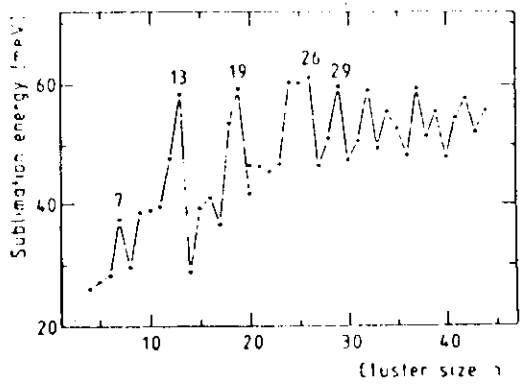

Figure 13 Sublimation energy calculated for Ar clusters.

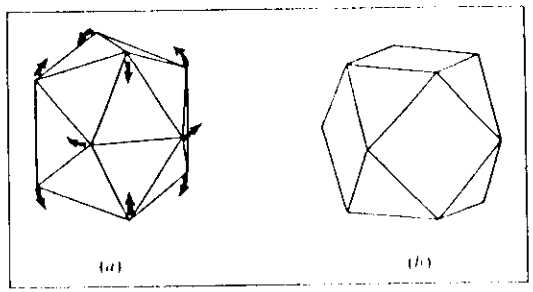

Figure 14 Transition from icosahedron (*a*) to cuboctahedron (*b*). By pulling the corners as indicated by the arrows it is possible to shift the icosahedral structure into a cuboctahedron.

TABLE 1 Some examples of magnetic particles obtained by chemical reaction.

Particles	Method
Fe_2O_3	$Fe^{2+}/Fe^{3+} + OH^-$
Fe_2O_3	Thermal decomp. of ferric solutions
FeC	Thermal decomp. of $Fe(CO)_5$
$Fe_{62}B_{38}$	Chemical reduction
$Fe_{37}Ni_{28}B_{34}$	Chemical reduction
$Fe_{44}Co_{19}B_{37}$	Chemical reduction
$Fe_{40}Cr_{16}B_{44}$	Chemical reduction
$Fe_{55}Mn_{20}B_{24}$	Chemical reduction
$SrFe_{12}O_{19}$	Ferrous hydroxide + Sr^{2+} + oxid.agent(90 °C)
$SrFe_{12}O_{19}$	Hydrolysis of metalorganic complexes
$Fe(OH)_nH_2O$	Precipitation

TABLE 3 : CLASSIFICATION OF BINDING IN CLUSTERS

TYPE	"CLASSICAL" GASES	NATURE OF BINDING	AVERAGE BINDING ENERGIES	REMARKS
VAN DER WAALS CLUSTERS	RARE GASES R_n $(N_2)_n$, $(CO_2)_n$ $(SF_6)_n$	DISPERSIVE ELECTROSTATIC	WEAK BINDING D ≤ 0.3 eV	AGGREGATES OF RARE GASES AND CLOSED-SHELL MOLECULES
MOLECULAR CLUSTERS	ORGANICS $(H)_n$ $(I_2)_n$	DISPERSIVE ELECTROSTATIC (NEAR VALENCE)	MODERATE BINDING D ≈ 0.3-1 eV	AGGREGATES OF ORGANIC MOLECULES AND SOME CLOSED-SHELL MOLECULES
HYDROGEN-BONDED CLUSTERS	$(HI)_n$, $(H_2O)_n$	H BONDING ELECTROSTATIC CHARGE TRANSFER	MODERATE BINDING D ≈ 0.3-0.5 eV	CLOSED SHELL MOLECULES CONTAINING H AND ELECTRO-NEGATIVE ELEMENTS
IONIC CLUSTERS	$(NaCl)_n$, $(CaF_2)_n$	IONIC BONDS CHARGE CHARGE INDUCED FORCES SHELL EFFECTS	STRONG BINDING D ≈ 2-4 eV	METALS FROM LEFT SIDE OF PERIODIC TABLE PLUS RIGHT SIDE ELECTRO-NEGATIVE ELEMENTS
VALENCE CLUSTERS	C_n, S_8, As_4	"CONVENTIONAL" CHEMICAL BONDS	STRONG BINDING D ≈ 1-4 eV	ISOMERIC MOLECULES AND RADICALS
METALLIC CLUSTERS	Na_n, Al_n, Cu_n, W_n	"METALLIC" BOND	MODERATE TO STRONG BINDING D ≈ 0.5-3 eV	WIDE OCCURRENCE IN THE LEFT OF B, Si, Ge, Sb, Pb IN ROWS 2-6 OF PERIODIC TABLE

	N_{max}	Y
Al_n	≈ 40	7 – 8
Si_n	11	3
Cu_n	> 100	11 – 15
Mo_n	≈ 30	7
W_n	≈ 20	7

Table 2 : Maximum number of atoms N_{max} in sputtered positively charged cluster ions (20 keV Xe^+, 100 $\mu A/cm^2$). In addition, theoretical and experimental sputtering yields Y are given for 20 keV Xe^+ bombardment.

Table 4. Magic numbers in mass spectra of van der Waals clusters which correlate with the numbers of atoms in closed shell (Mackay) icosahedra

	shell					
	1st	2nd	3rd	4th	5th	6th
model*	13	55	147	309	561	923
Ne	14	55/56				
Ar	(14)	m	148	309	561	923
Kr	(13)	m	147	309	561	923
Xe	13	55	147	309	561	923
CO	(13)	(55)	147	309		
CH_4	(14)	m	147	309		

Weak intensity anomalies are given in brackets, missing features are denoted by 'm'. * Closed shell icosahedra